Reevaluating hMT+ and hV4 functional specialization for motion and static contrast using fMRI-guided repetitive transcranial magnetic stimulation

Daniel Cohen McGill Vision Research, Department of Ophthalmology, McGill University, Montreal, Quebec, Canada

Erin Goddard McGill Vision Research, Department of Ophthalmology, McGill University, Montreal, Quebec, Canada

Kathy T. Mullen McGill Vision Research, Department of Ophthalmology, McGill University, Montreal, Quebec, Canada

Although visual areas hMT+ and hV4 are considered to have segregated functions for the processing of motion and form within dorsal and ventral streams, respectively, more recent evidence favors some functional overlap. Here we use fMRI-guided online repetitive transcranial magnetic stimulation (rTMS) to test two associated hypotheses: that area hV4 is causally involved in the perception of motion and hMT+ in the perception of static form. We use variations of a common global stimulus to test two dynamic motion-based tasks and two static form-based tasks in ipsilateral and contralateral visual fields. We find that rTMS to both hMT+ and hV4 significantly impairs direction discrimination and causes a perceptual slowing of motion, implicating hV4 in motion perception. Stimulation of hMT+ impairs motion in both visual fields, implying that disruption to one hMT+ disrupts the other with both needed for optimal performance. For the second hypothesis, we find the novel result that hV4 stimulation markedly reduces perceived contrast of a static stimulus. hMT+ stimulation also produces an effect, implicating it in static contrast perception. Our findings are the first to show that rTMS of hV4 can produce a large perceptual effect and, taken together, suggest a less rigid functional segregation between hMT+ and hV4 than previously thought.

Introduction

Human visual areas hMT+ and hV4 are regions within the dorsal and ventral processing streams, respectively, that have each been attributed with distinct visual specializations: global motion selectivity for hMT+ and shape processing for hV4 (Maunsell & Van Essen, 1983b; Newsome & Pare, 1988; Gallant, Braun, & van Essen, 1993; Born & Bradley, 2005; Rust, Mante, Simoncelli, & Movshon, 2006; Roe et al., 2012; Yue, Pourladian, Tootell, & Ungerleider, 2014). Although a conventional view of visual processing assumes the existence of neural substructures in extrastriate cortex with well-defined and independent functional properties, there is growing evidence against a strict segregation of function, indicative of more integrative processing with functional overlap between regions. Functional connectivity, for instance, is known to exist between ventral visual areas and the lateral temporal motion sensitive regions, for example, between MT and V2/V4 (Maunsell & Van Essen, 1983a; Ungerleider & Desimone, 1986; Walsh, Ellison, Battelli, & Cowey, 1998). Moreover, although motion inputs are undoubtedly processed in motion-sensitive cortical regions, such as MT, MST, and V3A (Zeki, 1974; Newsome & Pare, 1988; McKeefry, Burton, Vakrou, Barrett, & Morland, 2008), a range of findings suggest that ventral cortical regions may also be implicated in the perception of motion and appear to exhibit some degree of motion sensitivity (Ungerleider & Desimone, 1986; Newsome, 1997; P. Thompson, Brooks, & Hammett, 2006; Hayward, Truong, Partanen, & Giaschi, 2011). Results from nonhuman primates indicate that slower motion might be supported by the ventral pathway given the sustained nature of the parvocellular system, whereas faster motion may be supported by the more transient magnocellular pathway (Maunsell & Van Essen, 1983a; Ungerleider & Desimone, 1986; Ferrera, Nealey, &

Citation: Cohen, D., Goddard, E., & Mullen, K. T. (2019). Reevaluating hMT+ and hV4 functional specialization for motion and static contrast using fMRI-guided repetitive transcranial magnetic stimulation. *Journal of Vision, 19*(3):11, 1–20, https://doi.org/10.1167/19.3.11.

https://doi.org/10.1167/19.3.11 Received October 22, 2018; published March 27, 2019 ISSN 1534-7362

Maunsell, 1994; Lu, Chen, Tanigawa, & Roe, 2010). In addition, electrophysiology in macaque ventral cortex has revealed motion-selective pathways that project to ventral cortical regions with a significant proportion of neurons in V4 exhibiting direction selectivity (Desimone & Schein, 1987; Ferrera et al., 1994; Tolias, Sultan, et al., 2005; Gur & Snodderly, 2007; Schmid et al., 2013). Optical imaging has also shown macaque V4 to contain a columnar organization of motion-directional maps sensitive to changes in motion direction (Lu et al., 2010; An et al., 2012; Li et al., 2013). Conversely, there is less evidence to suggest that hMT+ might play a role in the perception of static stimuli. In fact, this area has provided some of the strongest evidence in favor of a functional specialization of brain areas. Nonetheless, the presence of orientation-selective neurons in MT that respond to static stimuli suggests that this area may not be invariant to static form (Maunsell & Van Essen, 1983b; T. D. Albright, 1984; Newsome & Pare, 1988; Khawaja, Liu, & Pack, 2013). Human fMRI also implies responses in hMT+ to static stimuli (O'Craven, Rosen, Kwong, Treisman, & Savoy, 1997).

The extent of any cross-functionality of these areas as they relate to human visual perception, however, has not been studied. To establish true cross-functionality, it is not sufficient to demonstrate cross-responsiveness but requires a demonstration of causal involvement in perception, for example, to show not only that hV4 responds to moving stimuli, but that the perception of moving stimuli depends on activity in hV4. Here we explore this directly for human vision by using fMRI-guided, online repetitive transcranial magnetic stimulation (rTMS) of areas hV4 and hMT+ in combination with psychophysical tasks. We test two associated hypotheses: that ventral area hV4 is involved in the processing of motion-based stimuli and that dorsal area hMT+ is involved in the processing of static form-based stimuli. We measure performance using four variations of a common global stimulus: two dynamic motion-based tasks (direction and speed discrimination) and two form-based tasks using static stimuli (orientation and contrast discrimination) applied to both the ipsilateral and contralateral visual fields (VFs). To address the first hypothesis, we establish the functional contribution of hMT+ to the motion-based tasks and compare with the contribution of hV4 to the same tasks. Although there is clinical evidence to suggest that ventral stream integrity may be necessary for uncompromised motion perception (Gilaie-Dotan et al., 2013), the role of ventral visual cortex in motion perception has not been demonstrated for normal human vision. For the second hypothesis, we first have to establish the contribution of hV4 to a form-based task. In general, the contribution of hV4 to visual perception by the application of rTMS is largely unexplored because it is harder to localize and more difficult to access in comparison to hMT+, requiring fMRI retinotopic mapping for each subject and online guidance to access its ventral cortical location. Here we aim to determine the contribution of hV4 to static, form-based tasks as well as any functional involvement of area hMT+ in these tasks. To our knowledge, this is the first attempt using rTMS to determine the contributions of area hV4 to both static form/contrast and dynamic motion and area hMT+ to static form processing. In determining the comparative roles of areas hMT+ and hV4 in the processing of motion and form, we provide new insights into the functional organization within extrastriate cortex.

Materials and methods

Participants

Seven healthy observers (four male, three female) participated in the present experiments. Five (all except S2 and S3) were naïve to the aims of the study. All had normal or corrected-to-normal visual acuity and no history of neurological and/or psychiatric disorders. Participants provided informed consent after being screened for contraindications and informed of safety risks associated with fMRI and TMS. Experiments were approved locally by the ethics review board of the Montreal Neurological Institute and conducted in accordance with the Declaration of Helsinki and established TMS safety protocols (Wassermann, 1998).

MRI and analysis

Functional T2* MR images were acquired on a 3T Siemens MAGNETOM Prisma system with a 32-channel head coil at the McConnell Brain Imaging Centre of the Montreal Neurological Institute. Gradient-echo pulse sequences were used to measure blood oxygenation level-dependent (BOLD) signal as a function of time (TR = 3,000 ms, TE = 30 ms, 39 axial slices, 1.5 mm^3 resolution). Localization of the human motion complex hMT+ was performed in a separate scan with identical spatial acquisition parameters (39 axial slices, 1.5 mm^3 resolution) and multiband acceleration factor of three (TR = 1,210 ms, TE = 30.4 ms). Acquired functional images were focused on visual cortex (partial brain coverage, including the entire occipital cortex, with slices oriented parallel to the calcarine sulcus). Head movement was limited by foam padding within the head coil. For each participant, two high-resolution, three-dimensional T1 images were acquired using an MP-RAGE sequence (TI = 900 ms,

TR = 2,300 ms, TE = 3.41 ms, 1.0 mm^3 resolution) and averaged to generate the participant's anatomical template.

The automatic segmentation processes from Freesurfer 6.0 (Dale, Fischl, & Sereno, 1999; Fischl, Sereno, & Dale, 1999) were used for each participant's template anatomical to define the gray/white matter and pial/gray matter boundaries. AFNI/SUMA packages (AFNI_17.2.12, September 6, 2017; Cox, 1996; Saad, Reynolds, Argall, Japee, & Cox, 2004) were used for all other MRI data processing. All functional data were preprocessed using slice-time correction and rigid-body motion correction before being aligned to the participant's template anatomical. Functional data were then projected onto the cortical surface by averaging between the white and pial boundaries and spatially smoothed (Gaussian filter, full-width at half maximum of 4 mm). Data collected during the phase-encoded retinotopic mapping scans (rotating wedge and expanding ring; see below for stimulus details) were analyzed using the AFNI script *@RetinoProc* (Saad, Ropella, Cox, & DeYoe, 2001). BOLD responses to the hMT+ localizer (see below) were modeled using a general linear model using the AFNI script *3dDeconvolve*, which, in addition to stimulus-related regressors, included regressors for linear and polynomial trends and six motion-correction parameters. Results from both the phase-encoded retinotopic mapping scans and the hMT+ functional localizer were visualized on inflated cortical representations using SUMA and used to define the regions of interest as detailed below (see Figure 1).

Identification and localization of target sites

Visual stimuli used for identification and localization of target sites were presented on a 32-in. BOLD screen by Cambridge Research Systems from a MacBook Pro laptop using Matlab (vR2017a) with routines from PsychToolbox (Brainard, 1997; Pelli, 1997). Participants viewed the BOLD screen, which was located at the rear of the MRI bore, through a mirror mounted on the head coil at a viewing distance of 125 cm. For each functional scan, participants were instructed to maintain fixation on a central marker while performing a simple fixation task.

The visual cortical regions V1, V2, V3, V3A/B, hV4, LO1, and LO2 were identified for each participant using rotating wedge stimuli and expanding and contracting concentric rings (Engel et al., 1994; Sereno et al., 1995) as described in previous work (Larsson & Heeger, 2006; Mullen, Dumoulin, McMahon, De Zubicaray, & Hess, 2007; Mullen, Thompson, & Hess, 2010) and in accordance with known anatomical landmarks (Figure 1A). Retinotopic mapping stimuli were presented within a central square of the BOLD screen with a width of 17.5° of visual angle. The area outside the stimulus was black. Participants were instructed to report the direction of a small arrow that appeared for 400 ms at a rate of approximately 1 Hz (with temporal jittering). All participants completed at least four repeats of the 6-min rotating wedge stimulus (two with clockwise and two with counterclockwise rotation) and one or two 6-min scans with the expanding and contracting ring stimuli.

The human motion complex hMT+ was identified using a localizer stimulus similar to that described previously (Dukelow et al., 2001; Huk, Dougherty, & Heeger, 2002). In a block-design paradigm, participants viewed 10-s blocks of moving and static dots interspersed with blank intervals (10 s duration). Moving and static dot stimuli comprised 2,000 low-contrast dots (10% contrast, half luminance increments and half luminance decrements), each with a circular, spatially smoothed Gaussian envelope with radius 0.33° on a background of mean gray luminance. Blank blocks consisted of a mean gray screen. During moving blocks, the dots moved smoothly toward or away from fixation at 8.4°/s with direction alternating at 1 Hz. In static blocks, randomly selected frames from the moving stimulus were presented and updated at 1 Hz. Moving and static dot locations were restricted to an annulus (inner diameter 3.5°, outer diameter 15.7°) with the remaining screen mean gray. Participants were instructed to indicate when the fixation marker changed from light gray to dark gray. Each participant completed one or two repeats of the 7.5-min hMT+ localizer. Two subjects (S3, S4) used an earlier version of the hMT+ localizer in which a low-contrast, flickering checkerboard (1%, 16 Hz, 15° diameter) was contrasted with a stationary version of the stimulus.

Coregistration of fMRI and TMS target sites

Stimulation sites were located within hMT+ and hV4 as functionally defined for each participant following the fMRI experiments described above (see Figure 1B and C). Target sites were located within either the left or right cerebral hemisphere. The right hemisphere was used as the initial stimulation site for all subjects. The left hemisphere was used in those participants who could not tolerate stimulation to the right hemisphere for reasons related to discomfort and/or twitching of facial nerves (three out of seven). For all target sites, we attempted to minimize depth relative to the cortical surface given that rTMS is maximally effective for superficial cortical targets.

Stimulation sites were targeted for functional disruption using the Brainsight neuronavigational system (Rogue Research, Inc., Montreal, Canada). Following

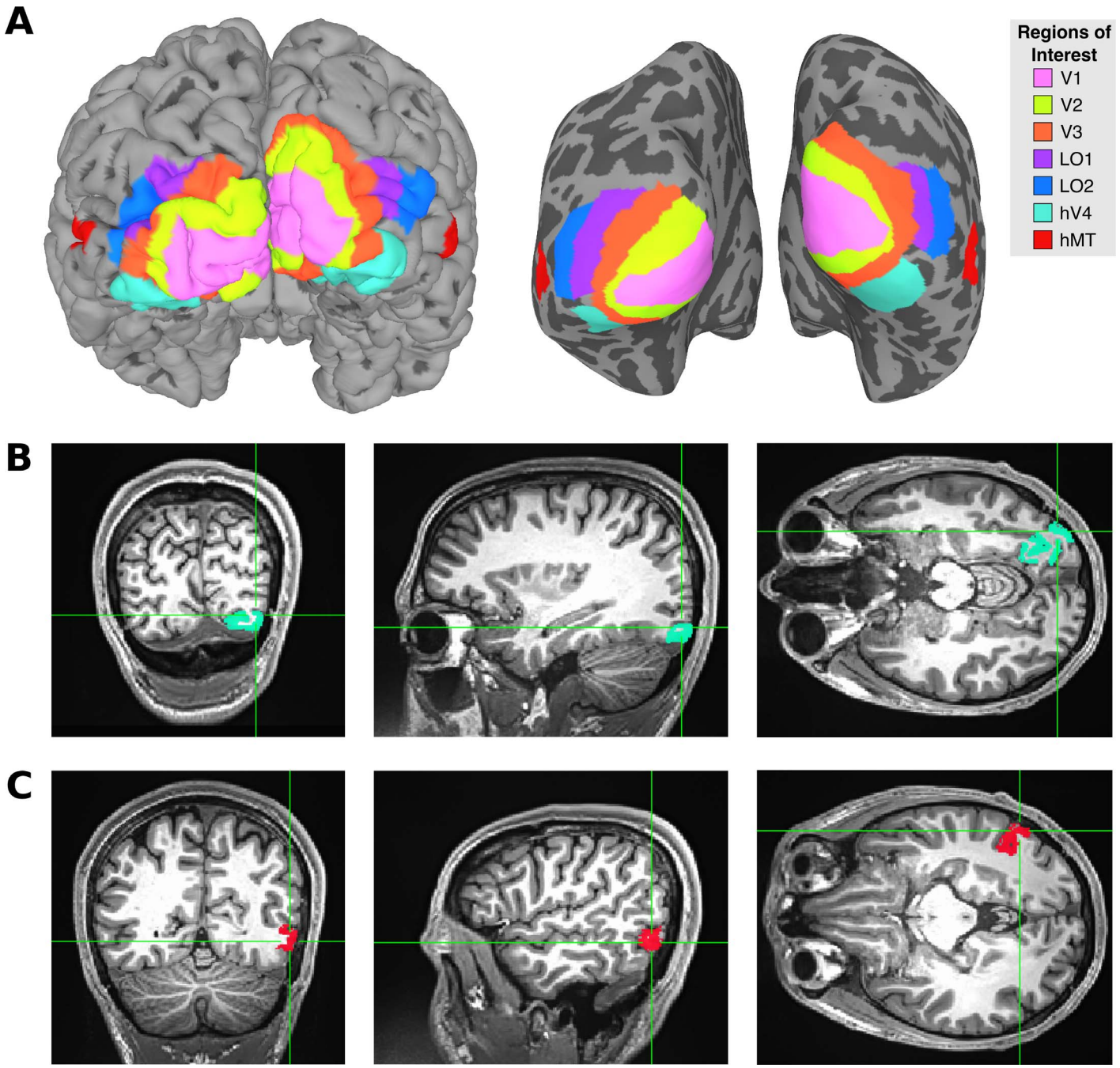

Figure 1. Functional and retinotopic identification of areas hV4 and hMT+ in one subject (S2). (A) The identification of regions of interest in the left and right hemispheres on a 3-D surface view (left) and on an inflated surface view (right). Bottom panels (B and C) show the areas identified as hV4 (B) and hMT+ (C) viewed on coronal, sagittal, and axial slices of the 3-D structural MRIs.

identification of target sites, structural and functional MR images were coregistered to a participant's head using a locally generated stereotaxic coordinate system, enabling the experimenter to link the spatial position of ultrasound transmitters on the subject and coil with prespecified landmarks on a 3-D representation of the subject's head. This allows for highly targeted positioning of the TMS coil relative to regions of interest where it can be maintained on a trial-by-trial basis.

Psychophysical apparatus

All stimuli were displayed on a high-resolution CRT monitor (1,280 × 1,024 pixels, 85-Hz frame rate; Mitsubishi Diamond Pro 2070SB). Stimuli were generated using Psykinematix v2.2 (KyberVision Japan LLC, Sendai, Japan) run on a MacBook Air laptop. Calibration of this equipment and linearization of the monitor's gamma function was performed using the

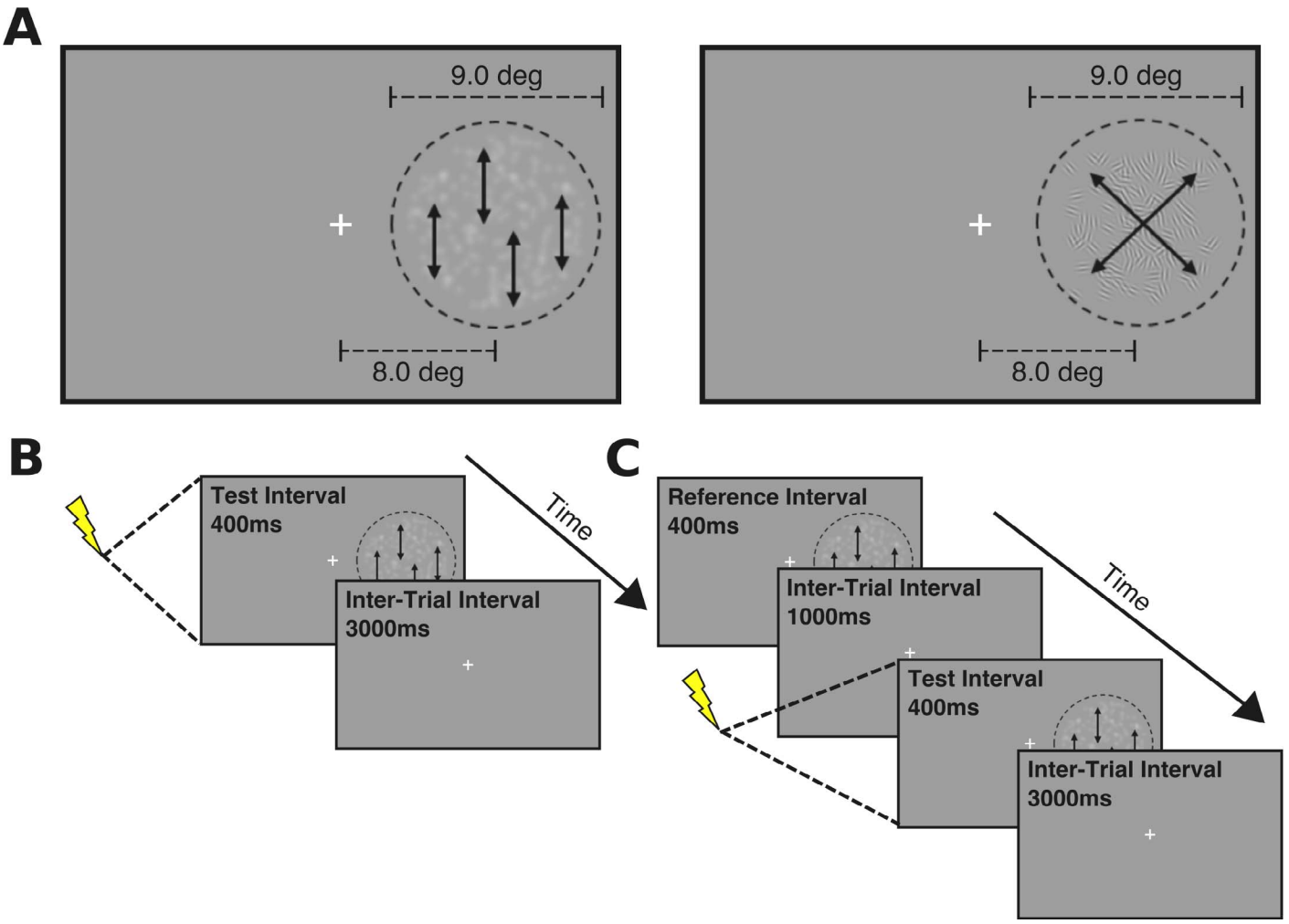

Figure 2. (A) An illustration of a frame of the dynamic random dot kinematogram used for the direction- and speed-discrimination tasks (left) and the static Gabor micropattern array used for the contrast- and orientation-discrimination tasks (right). (B) Temporal protocol for the single-interval direction- and orientation-discrimination tasks. (C) Temporal protocol for the two-interval speed- and contrast-discrimination tasks.

abovementioned software in combination with a Spyder5EXPRESS colorimeter (Datacolor, Inc., Lucerne, Switzerland). Responses were registered using a Cedrus RB-530 response box (Cedrus Corporation, San Pedro, CA). All stimuli were viewed binocularly in a dimly lit room at a viewing distance of 80 cm.

Psychophysical stimuli and tasks

We first measured performance on two dynamic motion-based tasks (direction and speed discrimination) with the speed-discrimination task allowing us to assess any TMS-induced changes in perceived speed. We then measured performance on two complementary static form-based tasks (orientation and contrast discrimination) with the contrast discrimination task allowing us to assess any TMS-induced changes in perceived contrast. As shown in Figure 2, all stimuli were composed of multiple elements randomly distributed within a circular aperture with a diameter of 9.0° of visual angle. Stimuli were presented against a uniform gray background (58.7 cd/m^2) at 8.0° of visual angle from central fixation in either the ipsilateral or contralateral VF relative to the hemisphere being stimulated. All stimuli were presented for a duration of 400 ms, presented within a Gaussian temporal envelope (sigma = 100 ms) with an intertrial interval of either 3,000 ms for single-interval tasks (Figure 2B) or an interstimulus interval of 1,000 ms and an intertrial interval of 3,000 ms for two-interval tasks (Figure 2C).

For all subjects, task-specific threshold performance measures were acquired in preliminary training sessions to establish values needed for a baseline performance level of approximately 80% correct. Methods for each task are described below. All subjects then underwent subsequent training to ensure that performance was consistent across fixation conditions (left and right

	Performance relative to baseline (% correct)	
	Decrement ($-\Delta$v or $-\Delta$cnt)	Increment ($+\Delta$v or $+\Delta$cnt)
Speed		
Perceived slowing	Improves	Deteriorates
Perceived speeding	Deteriorates	Improves
Loss of accuracy	Deteriorates	Deteriorates
Contrast		
Perceived reduction	Improves	Deteriorates
Perceived increase	Deteriorates	Improves
Loss of accuracy	Deteriorates	Deteriorates

Table 1. The principle of how to distinguish between a reduction in perceived speed/contrast, an increase in perceived speed/contrast, and a generalized loss of accuracy based upon the combined performance for both the decrement- and increment-discrimination tasks. *Note*: A perceptual change reflects a lateral shift in the underlying psychometric function and the point of subjective equality, whereas a loss of accuracy reflects a flattening of its slope.

VFs) and that any performance improvements with training had reached an asymptote (approximately 2 h of training per subject) prior to initiating rTMS.

Motion tasks

Stimuli for both motion-based tasks (speed and direction discrimination) were limited lifetime random dot kinematograms (Figure 2A). Motion sequences of 250 achromatic Gaussian blobs (sigma = 0.16°) were ramped on and off within the Gaussian temporal envelope. All motion was presented vertically (up/down). Motion coherence thresholds were acquired for direction-discrimination measurements, which depend upon the global integration of motion across the population of elements. We used a two-alternative, forced-choice (2AFC) staircase procedure with a fixed stimulus speed of 7.5°/s. Stimulus coherence was raised by 25% of the previous coherence value following an incorrect response and lowered by 12.5% following two consecutive correct responses. The overall threshold value used for subsequent training was calculated as the arithmetic mean of the last five reversals, yielding a threshold level of 79% correct with a minimum of five staircases run per fixation condition. Auditory feedback was given on correct responses only during training sessions with no auditory feedback given throughout subsequent rTMS.

For speed-discrimination measurements, motion coherence was fixed at 80%. Speed-discrimination thresholds were acquired using a method of constant stimuli (MCS) in conjunction with a two-interval, forced-choice (2IFC) procedure. The participant's task was to indicate in which of two intervals the stimulus appeared to be moving faster. A fixed reference speed of 7.5°/s was always presented in the first interval given the rTMS protocol described below. For each participant, we determined the speed difference at which they could perform the speed-discrimination judgement at a performance level of 80% correct. Two conditions, a speed decrement ($+\Delta$v) and a speed increment ($-\Delta$v) relative to the reference speed were run simultaneously (see Table 1). By measuring differential changes in the ability to distinguish speed increments and decrements from the fixed reference speed, we were able to differentiate a perceived change in stimulus speed (increase or decrease) from an overall loss in accuracy.

Form tasks

Stimuli for both static form-based tasks (orientation and contrast discrimination) consisted of arrays of 100 Gabor micropatterns (sigma = 0.20°) presented for 400 ms (Figure 2A). The spatial frequency of the sinusoidal modulation within the Gabor was set at 0.40 c/°. For orientation-discrimination measurements, the orientation of each Gabor micropattern was selected from a Gaussian distribution with a variable mean of either 45° (right oblique) or 135° (left oblique) as described previously (Mansouri, Hess, & Allen, 2007), such that the distribution's variance could range from 10° (almost all elements aligned) to 100° (high orientation variability). The task requires the integration of orientation across the population of elements. The element contrast was fixed at 45%. A 2AFC staircase procedure, analogous to that used for direction-discrimination measurements, was used to acquire orientation-discrimination thresholds. The first reversal within the staircase procedure was taken as an estimate of the threshold level, after which the stimulus coherence was raised by 8% following an incorrect response or lowered by 4.5% following two consecutive correct responses. The overall threshold value used for subsequent training was calculated as the arithmetic mean of the last five reversals, yielding a threshold level of 79% correct with a minimum of five staircases run per fixation condition. As with motion-based tasks, auditory feedback was given on correct responses only during training sessions and not throughout subsequent rTMS.

For contrast-discrimination measurements, the distribution's orientation variance was fixed at 40°, and contrast was set according to individual threshold values as described below. Contrast-discrimination thresholds were acquired using a MCS in conjunction with a 2IFC procedure analogous to that used for speed-discrimination measurements. The participant's task was to indicate in which of the two intervals the stimulus appeared to have a higher contrast. A fixed reference contrast of 45% was always presented in the

first interval given the rTMS protocol described below. For each participant, we determined the contrast difference at which they could perform the contrast-discrimination judgement at a performance level of 80% correct. Two conditions, a contrast decrement and increment (relative to the reference contrast) were run simultaneously, following a protocol analogous to that employed for the speed-discrimination task (see Table 1). Following the acquisition of threshold measurements, further practice trials were run for each of the four tasks to confirm the stimulus magnitudes required to maintain a performance level near 80% correct. These magnitudes were then used in the subsequent rTMS protocol as outlined below.

TMS protocol

Online repetitive TMS was applied as a train of five biphasic pulses using a figure-of-eight coil (70 mm diameter) connected to a MagVenture magnetic stimulator (MagVenture, Inc., Farum, Denmark). The coil was placed over the scalp tangentially with the handle oriented upward. rTMS trains were applied at a frequency of 12.5 Hz, yielding five pulses over the 400-ms stimulus presentation and at 65% of the maximum stimulator output, a typical intensity for stimulation of visual regions. One subject (S4) required a reduced level (55%) due to strong discomfort; however, the effect sizes obtained were no different from those of the other subjects. rTMS was delivered concurrent with stimulus onset as previous results have demonstrated this temporal configuration to be most effective at inducing effects in hMT+ (McKeefry et al., 2008) (see Figure 2B and C). No feedback was given throughout rTMS sessions.

In every rTMS session, participants completed four stimulus blocks consisting of 50 trials per block. Two blocks were run prior to rTMS to determine the baseline level of performance, after which two blocks of rTMS were run for each of the target sites (hMT+ or hV4) and presentation conditions (ipsilateral or contralateral VF). Sessions for each target site and presentation condition were randomized and run on separate days. Throughout all subsequent analyses, baseline performance for each task was averaged across sessions separately for each of the contralateral and ipsilateral VFs. Statistical analyses were performed using SPSS version 22 (IBM Corp., Armonk, NY), and a false discovery rate (FDR) criterion (Benjamini & Hochberg, 1995) was used to correct for multiple comparisons for each experiment. For FDR correction, statistical tests for Experiments 1 and 5 (both direction-discrimination tasks) were corrected as a group.

Results

Experiment 1: Effect of rTMS on direction discrimination

For the first motion-based task, we measured the effect of rTMS to either hMT+ or hV4 on the percentage of correct responses for direction discrimination of the global motion stimulus. Figure 3 shows performance on the direction-discrimination task with and without rTMS for area hMT+ (in red) and area hV4 (in blue). Performance data during rTMS were collapsed across sessions for the seven subjects (dark bars) and compared with baseline performance (light bars). A series of paired-sample t tests with FDR correction indicate that mean performance following rTMS to hMT+ was significantly lower than baseline in both the contralateral, $t(6) = 6.373$, $p = 0.001$, $q < 0.01$, $d = 2.31$, and ipsilateral, $t(6) = 5.605$, $p = 0.001$, $q < 0.01$, $d = 2.08$, VFs as well as in hV4 for the contralateral VF, $t(6) = 3.109$, $p = 0.021$, $q < 0.05$, $d = 1.12$. Each of these effects exceeded Cohen's (1988) convention for a large effect ($d = 0.80$). For stimuli presented in the ipsilateral VF, stimulation of hV4 did not yield significant changes from baseline, $t(6) = 1.088$, $p = 0.318$, $d = 0.39$. These results indicate that stimulation of area hMT+ leads to a bilateral impairment in the ability to discriminate motion direction, whereas stimulation of hV4 leads to comparable deficits but only in the contralateral VF. That bilateral VF deficits were observed only for hMT+ and not hV4 rules out any artifactual effects based upon variations in fixation or the subject making eye movements to the test stimulus.

Experiment 2: Effect of rTMS on speed discrimination

We next considered whether the involvement of our two target areas would generalize to the second motion task (speed discrimination/perception). We measured the percentage of correct responses for the task of discriminating which is the faster of two sequential stimuli, presented in a 2IFC design. Two conditions were run simultaneously with a fixed reference stimulus paired with either a slower (speed decrement, $-\Delta v$) or faster test stimulus (speed increment, $+\Delta v$). Table 1 shows how speed-discrimination measurements for increments and decrements allow us to determine whether there has been a change in perceived speed (faster vs. slower) or a generalized loss of accuracy in discrimination. If perceptual slowing occurs during the application of rTMS in the test interval, performance for the discrimination of the speed decrement (slower test stimulus from a fixed reference stimulus) improves because the

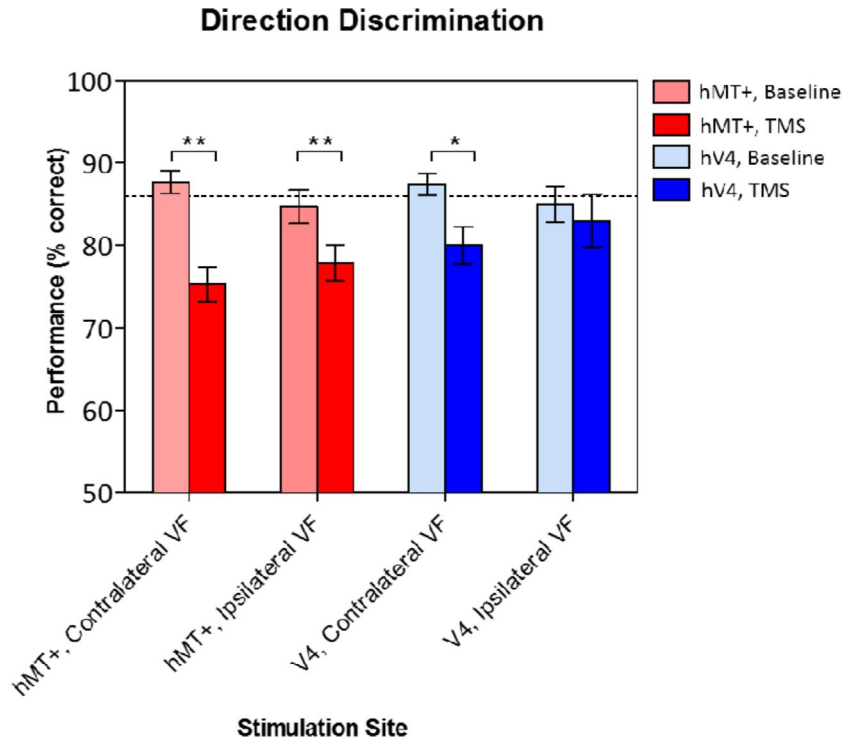

Figure 3. Effect of rTMS on performance of direction-discrimination task ($n = 7$). Figure shows mean performance as percentage correct as a function of stimulation site. Dotted lines indicate the average of the baseline conditions (86% correct). Error bars represent the standard error of the mean. VF = visual field. *$q < 0.05$. **$q < 0.01$ (FDR corrected).

perceptual slowing of the slower test stimulus effectively increases the size of the perceptual difference between intervals, whereas performance for the discrimination of the speed increment (faster test stimulus from a fixed reference stimulus) deteriorates because the perceptual slowing of the faster test stimulus effectively decreases the perceptual difference. The reverse would occur if rTMS causes perceived speed to increase. However, if rTMS leads to an overall loss of accuracy in the ability to discriminate stimulus speed, then performance on both discriminations, the increment and decrement, would be expected to get worse.

Figure 4 shows performance on the speed-discrimination task with and without rTMS for area hMT+ (in red) and area hV4 (in blue). Performance data during rTMS were collapsed across sessions for the seven subjects (dark bars) and compared with baseline performance (light bars). Figure 4A (left panel) shows performance on the speed-decrement task. A series of paired-sample t tests with FDR correction indicate that mean performance following rTMS to hMT+ was significantly higher than baseline in both the contralateral, $t(6) = -4.192$, $p = 0.006$, $q < 0.05$, $d = 1.58$, and ipsilateral, $t(6) = -3.814$, $p = 0.009$, $q < 0.05$, $d = 1.46$, VFs, indicating an improvement in the discrimination of speed decrements. Stimulation of hV4 did not yield any significant changes from baseline in either the contralateral, $t(6) = -1.611$, $p = 0.158$, $d = 0.61$, or ipsilateral, $t(6) = 1.337$, $p = 0.230$, $d = 0.50$, VFs. Figure 4A (right panel) shows performance on the speed-increment task. Mean performance here was significantly lower than baseline across all stimulation sites, including hMT+ in both the contralateral, $t(6) = 4.968$, $p = 0.003$, $q < 0.01$, $d = 1.86$, and ipsilateral, $t(6) = 6.032$, $p = 0.001$, $q < 0.01$, $d = 2.27$, VFs as well as hV4 in the contralateral, $t(6) = 4.012$, $p = 0.007$, $q < 0.05$, $d = 1.52$, and ipsilateral, $t(6) = 3.926$, $p = 0.008$, $q < 0.05$, $d = 1.47$, VFs, indicating a loss in the discrimination of speed increments across all conditions.

As it is a dissociation of performance on speed increments and decrements that indicates a perceptual change in speed during rTMS, Figure 4B plots the speed-discrimination data as the percentage change from baseline for the speed decrements and increments for both target areas (hMT+, red bars and hV4, blue bars). The combination of improved performance for the speed decrement and reduced performance for the speed increment is consistent with a perceived slowing of the test stimulus during rTMS. Paired-sample t tests with FDR correction were used to compare performance differences between speed increments and decrements with the data illustrating that rTMS to hMT+ leads to a perceptual slowing of motion in both the ipsilateral, $t(6) = 6.389$, $p = 0.001$, $q < 0.01$, $d = 2.42$, and contralateral, $t(6) = 4.837$, $p = 0.003$, $q < 0.01$, $d =$

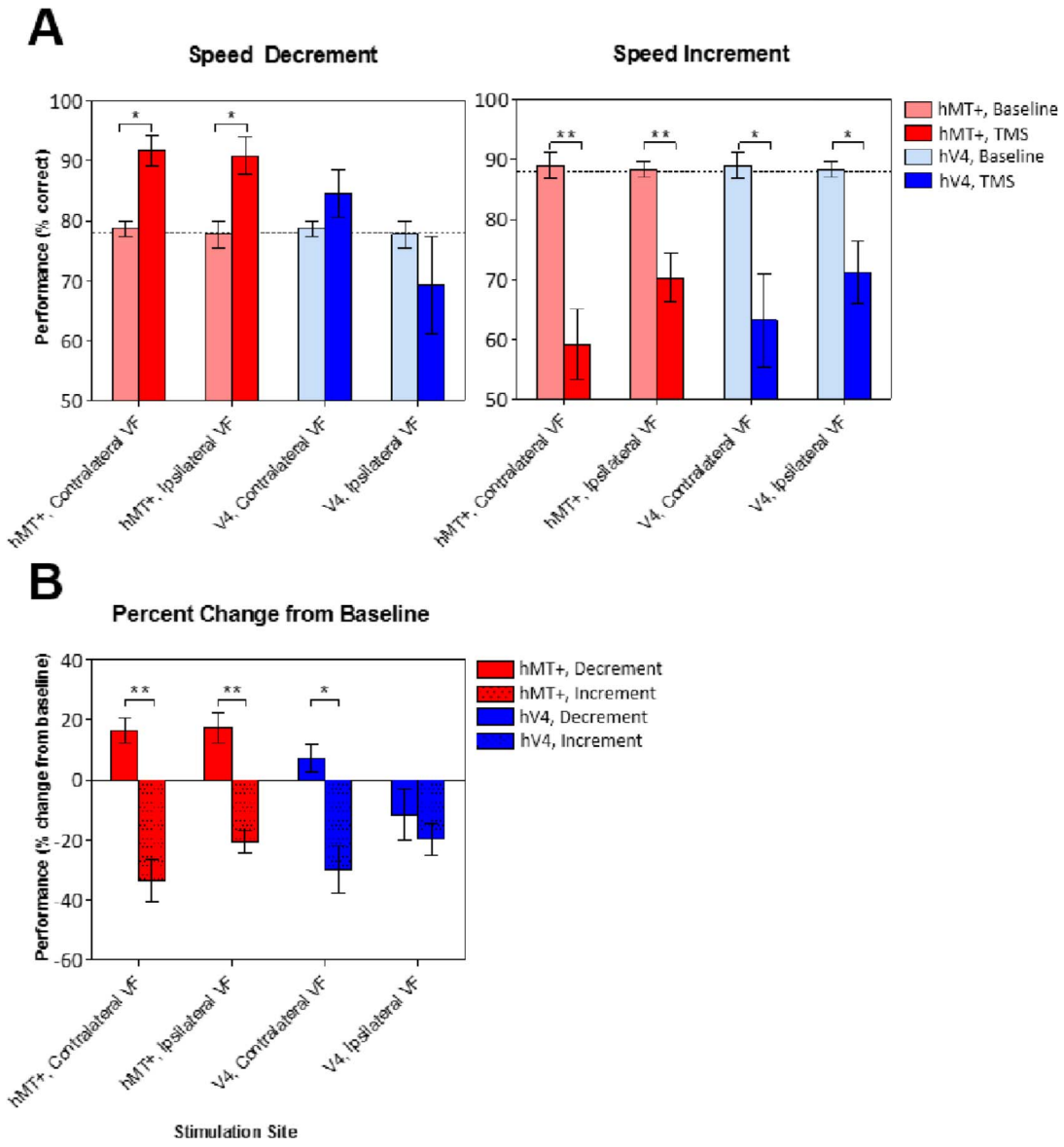

Figure 4. Effect of rTMS on performance of speed-discrimination task ($n = 7$). (A) Mean performance as percentage correct as a function of stimulation site for the speed decrement (left) and increment (right). Dotted lines indicate the average of the baseline conditions (speed decrement = 79% correct, speed increment = 88% correct). (B) Percentage change in performance relative to baseline for both the speed decrement and increment. Error bars represent standard error of the mean. VF = visual field. *$q < 0.05$. **$q < 0.01$ (FDR corrected).

1.83, VFs as well as hV4 in the contralateral VF, $t(6) = 3.133$, $p = 0.020$, $q < 0.05$, $d = 1.18$. For stimuli presented in the ipsilateral VF, stimulation of hV4 appears to lead to a small generalized reduction of accuracy with no evidence for perceived slowing of stimulus speed, $t(6) = 0.655$, $p = 0.537$, $d = 0.25$.

Experiment 3: Effect of rTMS on contrast discrimination

Here we used stimuli designed to elicit preferential responses in ventral cortical regions to functionally target the role of area hV4. We measured the percentage of correct responses for the task of discriminating which of two sequentially presented stimuli appear to have the higher contrast. The method is exactly analogous to that employed for the speed-discrimination task with two conditions run simultaneously and a fixed reference contrast paired with either a lower contrast test (contrast decrement, −Δ cnt) or a higher contrast test (contrast increment, +Δ cnt) (see Table 1). If a perceptual reduction of the test stimulus contrast occurs during application of rTMS, performance for the discrimination of the contrast decrement improves because the reduction in

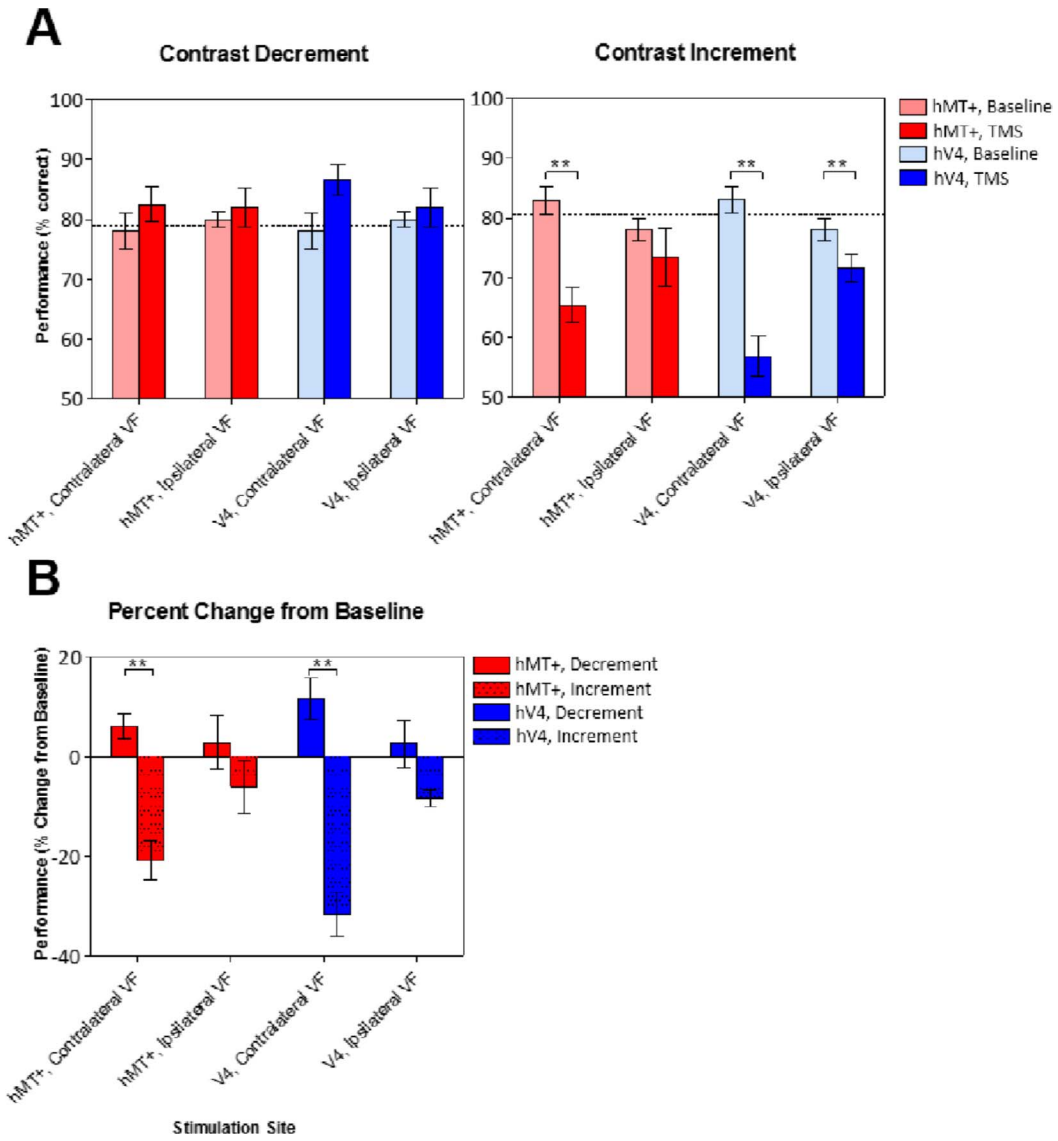

Figure 5. Effect of rTMS on performance of contrast-discrimination task ($n = 7$). (A) Mean performance as percentage correct as a function of stimulation site for the contrast decrement (left) and increment (right). Dotted lines indicate the average of the baseline conditions (contrast decrement = 79%, contrast increment = 81% correct). (B) Percentage change in performance relative to baseline for both the contrast decrement and increment. Error bars represent standard error of the mean. VF = visual field. *$q < 0.05$. **$q < 0.01$ (FDR corrected).

perceived contrast of the lower contrast test stimulus effectively increases the contrast decrement, whereas performance for the discrimination of the contrast increment deteriorates because the reduction in perceived contrast of the higher contrast test stimulus effectively decreases the contrast increment. The reverse would occur if rTMS caused an increase in perceived contrast. If an overall loss of accuracy in the ability to discriminate between contrast values occurs, then both increment and decrement discriminations would be expected to get worse.

Figure 5 shows performance on the contrast-discrimination tasks with and without rTMS for area hMT+ (in red) and area hV4 (in blue). Performance data during rTMS were collapsed across sessions for the seven subjects (dark bars) and compared with baseline performance (light bars). Figure 5A (left panel) shows performance on the contrast-decrement task. A series of paired-sample t tests with FDR correction indicate there were no significant changes from baseline for stimuli presented in the contralateral VF following rTMS of either hMT+, $t(6) = -2.606$, $p = 0.040$, $q > 0.05$, $d = 0.99$, or hV4, $t(6) = -2.956$, $p = 0.025$, $q > 0.05$, $d = 1.12$, or for stimuli presented in the ipsilateral VF for either hMT+, $t(6) = -0.493$, $p = 0.640$, $d = 0.19$, or hV4, $t(6) = -0.544$, $p = 0.606$, $d = 0.21$. For the contrast increment task (Figure 5A, right panel), mean performance following rTMS to hMT+ was signifi-

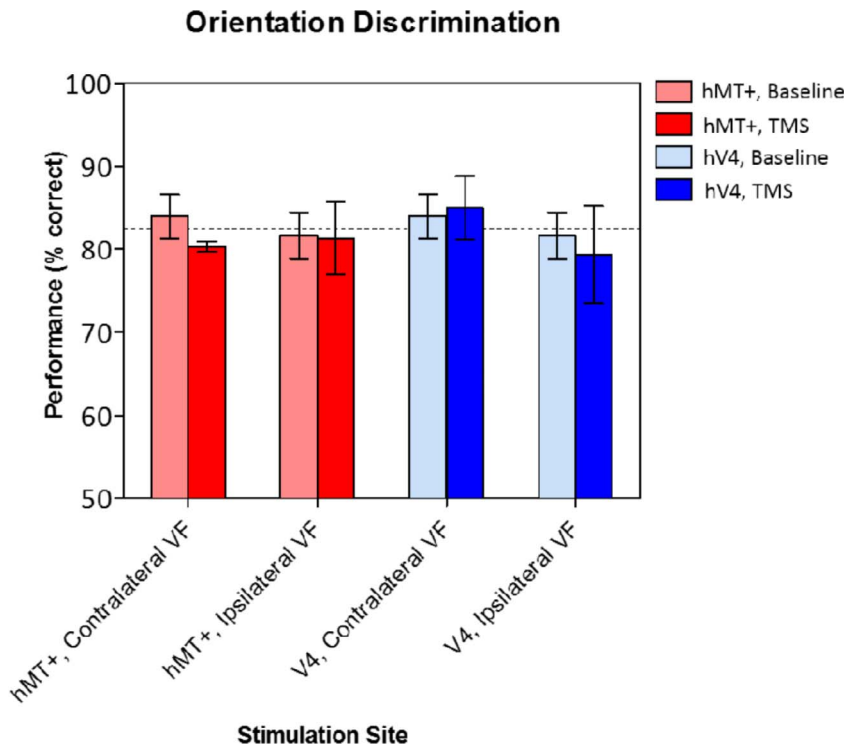

Figure 6. Effect of rTMS on performance of orientation-discrimination task ($n = 3$). Figure shows mean performance as percentage correct as a function of stimulation site. Dotted lines indicate the average of the baseline conditions (83% correct). Error bars represent the standard error of the mean. VF = visual field.

cantly lower than baseline in the contralateral VF, $t(6) = 5.024$, $p = 0.002$, $q < 0.01$, $d = 1.90$, only with no deficit found for stimuli presented in the ipsilateral VF, $t(6) = 1.105$, $p = 0.311$, $d = 0.42$. For hV4, rTMS lead to a large reduction in mean performance for stimuli presented in the contralateral VF, $t(6) = 6.930$, $p = 0.0004$, $q < 0.01$, $d = 2.65$, and a smaller deficit for the ipsilateral VF, $t(6) = 4.982$, $p = 0.002$, $q < 0.01$, $d = 1.88$.

To reveal a dissociation of performance on contrast increments and decrements indicative of a perceptual change in contrast, Figure 5B shows the data plotted as a percentage change from baseline for both the contrast decrement and increment for the two target areas (hMT+ in red and hV4 in blue). The combination of a performance increase for the contrast decrement and a performance loss for the contrast increment reflects a perceived reduction of the test contrast. Paired-sample t tests with FDR correction were used to compare performance differences between contrast increments and decrements with the data illustrating that rTMS to both hV4, $t(6) = 6.349$, $p = 0.001$, $q < 0.01$, $d = 2.40$, and hMT+, $t(6) = 5.436$, $p = 0.002$, $q < 0.01$, $d = 2.06$, leads to a significant reduction in perceived contrast in the contralateral VF with hV4 showing the greatest effect. For stimuli presented in the ipsilateral VF, stimulation of neither hMT+, $t(6) = 0.973$, $p = 0.368$, $d = 0.37$, nor hV4, $t(6) = 1.960$, $p = 0.098$, $d = 0.74$, yielded any significant changes between conditions.

Experiment 4: Effect of rTMS on orientation discrimination

Finally, we tested a second static task designed to elicit preferential responses in ventral cortical regions. We measured the effect of rTMS of our two target areas on the ability to discriminate between the orientation of static elements. Our methods were analogous to those employed for the motion-coherence/direction-discrimination task except that here participants were required to judge which way the stimulus appears to be oriented. Figure 6 shows performance on orientation discrimination with and without rTMS for our two target areas for an initial three subjects. Performance data during rTMS were collapsed across sessions for three subjects (dark bars) and compared with baseline performance (light bars). A series of paired-sample t tests with FDR correction indicate that rTMS to hMT+ yielded no significant changes from baseline for stimuli presented in the contralateral, $t(2) = 1.808$, $p = 0.212$, $d = 1.00$, or ipsilateral, $t(2) = 0.152$, $p = 0.893$, $d = 0.05$, VFs, nor did rTMS to hV4 in either the contralateral, $t(2) = -0.199$, $p = 0.861$, $d = 0.13$, or ipsilateral, $t(2) =$

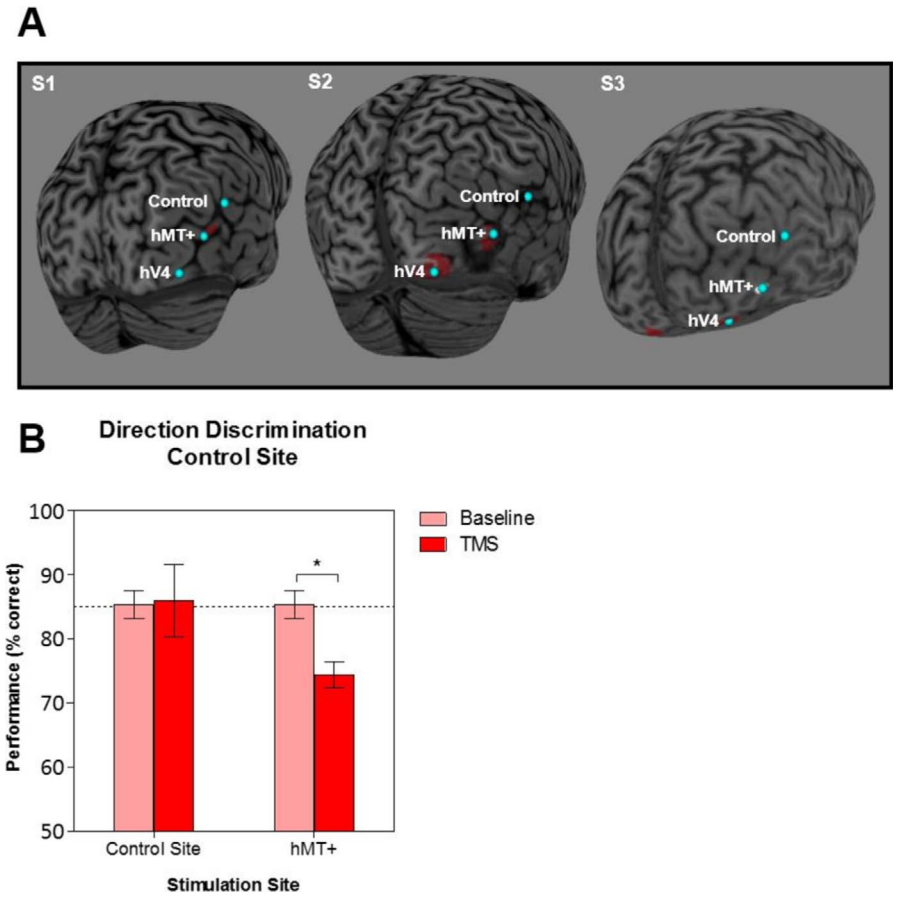

Figure 7. Control for lateral spread of rTMS effects. (A) Location of the control region adjacent to hMT+ in three participants. (B) Mean performance as percentage correct relative to baseline on the direction-discrimination task using both the non-hMT+ stimulation site and hMT+ for the same subjects ($n = 3$) for stimuli presented in the contralateral VF. Dotted lines indicate the average of the baseline conditions for all stimuli presented in the contralateral VF (85% correct). Error bars represent the standard error of the mean. *$q < 0.05$ (FDR corrected).

0.469, $p = 0.685$, $d = 0.26$, VFs. To control for the possibility that orientation-discrimination judgements may be made more rapidly than those for motion tasks during the early part of the stimulus presentation, we shortened the duration of the stimulus presentation to 100 ms (from 400 ms) and increased the frequency of stimulation to 25 Hz (from 12.5 Hz). Even with the shorter stimulus duration and more frequent pulses, we found that rTMS to hV4 yielded no significant changes from baseline for stimuli presented in either the contralateral and ipsilateral VFs. We subsequently discontinued the orientation-discrimination experiment because it failed to show an effect in hV4 (or hMT) in our initial subset of participants, and a power analysis indicated that, even for the largest estimated effect size ($d =$ 1.00 for contralateral hMT), we would require an unfeasibly large number of subjects ($n = 16$ without FDR correction) to detect a genuine effect of this magnitude.

Experiment 5: Control for lateral spread of rTMS effects

To examine the spatial selectivity of rTMS effects, we conducted a control experiment in which we apply stimulation to a control region adjacent to area hMT+. Given our interest in the involvement of area hV4 in motion perception (and area hMT+ in static form perception), we want to ensure that effects observed in one region are not simply a result of the passive spread of stimulation across the cortical surface. Such controls for the lateral spread of rTMS effects are performed by moving the coil 1–2 cm away from the primary site of stimulation (McKeefry et al., 2008; Silson et al., 2013). Here we measure the effects of rTMS on the performance of the direction-discrimination task after moving the stimulation site approximately 2 cm from the functionally defined hMT+ (see Figure 7A) a similar distance from hMT+ as hV4 but in a different direction. Performance on the direction-discrimination

task for stimuli presented in the contralateral VF is shown in Figure 7B. Performance data during rTMS were collapsed across sessions for three subjects (dark bars) and compared with baseline performance (light bars). Baseline performance was averaged across all sessions for which stimuli were presented in the contralateral VF. A paired-samples t test with FDR correction indicates that stimulation of the control site induced no significant deficits in performance relative to baseline, $t(2) = -0.160$, $p = 0.888$, $d = 0.08$, suggesting that the passive spread of stimulation across the cortical surface from the control site does not reach and affect hMT+ and implying that effects observed in area hV4 for the previous tasks were not due simply to the indirect spread of stimulation to area hMT+ (and vice versa). For comparison purposes, group-averaged performance data following rTMS to hMT+ for the same subjects are included, $t(2) = 7.201$, $p = 0.019$, $q < 0.05$, $d = 4.40$.

Discussion

This study set out to explore the relative contributions made by areas hMT+ and hV4 to the perception of motion and static form and the extent of any cross-functionality between these two target regions. To this end, we determined the effect of fMRI-guided rTMS of areas hMT+ and hV4 on two motion tasks and two static form-based tasks, tested using similar multielement stimuli in both ipsilateral and contralateral VFs. We find that rTMS to both visual areas significantly impairs performance on the direction-discrimination task and leads to a perceptual slowing. Stimulation of hMT+, however, produces a bilateral impairment in both the contralateral and ipsilateral VFs, whereas rTMS to hV4 impairs motion only in the contralateral VF. For the static form-based tasks, perceived contrast is reduced following stimulation of both areas but only in the contralateral VF with the greatest effect found in hV4. Orientation discrimination is not affected by rTMS for any of the stimulation conditions.

The implications of these results are threefold. First, the results obtained on the direction- and speed-discrimination tasks demonstrate that area hMT+ contains a bilateral VF representation for motion-based tasks. As we find no effects in the ipsilateral VF for the contrast-discrimination tasks, this bilaterality is effectively limited to motion processing. Second, our results demonstrate that rTMS of hV4 leads to a reduction in perceived contrast for stimuli presented in the contralateral VF, the largest effect in all our results, and in an area that has been virtually unexplored to date. Third, they provide evidence of cross-functionality between hMT+ and hV4. We find that stimulation of hV4 impairs performance on motion-based tasks although only for stimuli presented in the contralateral VF, an effect that may be mediated indirectly through disruption of the functional connectivity between hMT+ and hV4 or by direct impairment of functional motion processing in hV4. Moreover, stimulation of hMT+ affects static contrast perception in the contralateral VF. Taken together, these findings demonstrate some convergence of function between hMT+ and hV4 and support the presence of integrative processing and functional cross-talk between these areas as opposed to the modular functional segregation typical of the classic models of visual perception.

The bilateral role of hMT+ in motion processing

Motion perception has proven particularly amenable to study via rTMS (Walsh et al., 1998; Cowey, Campana, Walsh, & Vaina, 2006; McKeefry et al., 2008; Stevens, McGraw, Ledgeway, & Schluppeck, 2009; McKeefry, Burton, & Morland, 2010; Waterston & Pack, 2010; Kaderali, Kim, Reynaud, & Mullen, 2015; Liu & Pack, 2017; Pavan, Ghin, Donato, Campana, & Mather, 2017; Strong et al., 2017). We used global motion stimuli in order to best target area hMT+ given that global motion requires signal integration across all elements of the stimulus, and area hMT+ is known to play a principal role in the spatial integration of local motion to reveal global motion direction (Born & Bradley, 2005). Consistent with this, we found that rTMS of hMT+ caused impairments in the ability to use motion coherence in estimating motion direction. However, only a handful of studies have focused on the processing of speed. Here, by showing differential changes in performance on speed increments and decrements, we were able to demonstrate a perceptual slowing in area hMT+, results that are complementary to previous findings obtained using similar rTMS protocols for nonglobal, grating stimuli (McKeefry et al., 2008; McKeefry et al., 2010). Interestingly, there is a similar loss of direction discrimination for global motion stimuli as well as a perceptual slowing for gratings when hMT+ is "impaired" by the use of luminance noise masking of isoluminant chromatic stimuli (Mullen, Yoshizawa, & Baker, 2003; Michna & Mullen, 2008).

Notably, stimulation of hMT+ led to perceptual impairments in both the ipsilateral and contralateral VFs. Different subdivisions of hMT+ have been identified on the basis of retinotopic organization and receptive field properties (Dukelow et al., 2001; Huk et al., 2002; Amano, Wandell, & Dumoulin, 2009). One subregion (putative MT) is not thought to respond to ipsilateral stimulation, indicative of smaller receptive field sizes, whereas the other (putative MST) responds

to stimuli in both the ipsilateral and contralateral visual fields, indicative of larger receptive field sizes. Our fMRI localizer for hMT+ (15° diameter) was centrally fixated allowing for both contralateral and ipsilateral functional responses. Indeed, receptive fields of macaque MST neurons (but not MT neurons) often extend >10° into the ipsilateral hemifield relative to the vertical meridian (Ungerleider & Desimone, 1986; T. Albright & Desimone, 1987; Komatsu & Wurtz, 1988). Our bilateral effects observed in hMT+ are, therefore, likely mediated by neurons in area MST. To our knowledge, we are among the first to demonstrate causal bilateral function in hMT+ motion processing using rTMS. Selective rTMS stimulation of the contralateral VFs of MT and MST has previously been used to explore differences in the types of preferred motion between the subdivisions of hMT+ with Strong et al. (2017a) showing the up/down motion used here is common to both subdivisions. Differential VF effects have also been reported between the left and right cerebral hemispheres, in which stimulation of the right hemisphere produced bilateral motion processing deficits but left-hemisphere stimulation produced only contralateral impairments (Thakral & Slotnick, 2011; Strong et al., 2017b). Contrary to these results, however, we find bilateral deficits in our motion tasks following rTMS to both the right and left cerebral hemispheres. This might be due to methodological differences. To test both VFs, we varied the VF location of the stimulus while stimulating one hemisphere, which avoids the intrasubject variability based on differences in region of interest localization and stimulation between a subject's two hemispheres, which can occur when stimulation is switched between the left and right hemispheres with the stimulus remaining in one VF.

Our demonstration of a functional projection from the ipsilateral VF to hMT+ has several interesting implications. First, the fact that we see an rTMS-induced deficit in the ipsilateral VF of the stimulated hMT+ is curious given that there is an unstimulated, normally functioning hMT+ in the contralateral hemisphere that is also "seeing" the motion stimulus. Hence, the impairment of motion processing in the ipsilateral field implies that we require two functioning hMT+s (left and right) for normal motion performance. In other words, it appears that there is a kind of "compulsory cross-talk" between left and right hMT so that disruption to one necessarily disrupts the other. These results lead to direct predictions for psychophysical testing. Second, the functional presence of the ipsilateral VF projection to hMT+ that we have demonstrated has interesting implications for cortically blind subjects. Whether the ipsilateral projection is via the superior colliculus and pulvinar nuclei or is callosal (Leh, Ptito, Schönwiesner, Chakravarty, & Mullen, 2010; Ajina, Pestilli, Rokem, Kennard, & Bridge, 2015), a functioning ipsilateral projection may potentially provide access of the "blind" VF to motion processing in the healthy hemisphere when contralateral early visual areas are damaged.

The role of hV4 in motion processing

The perceptual impairments present in the motion tasks following stimulation of hV4 suggest that motion perception relies on a combination of dorsal and ventral contributions with ventral regions displaying a degree of influence on the visual attributes of motion direction and speed. The idea that motion perception involves ventral cortical regions runs counter to the modular view, in which motion inputs are thought to be processed in functionally distinct dorsal regions. Recent clinical evidence, however, shows widespread impaired motion perception in five patients with ventral cortical lesions, particularly in right hemispheres, supporting a closer interplay between motion processing and ventral visual cortex (Gilaie-Dotan et al., 2013). In primate studies, there is considerable evidence for directionally selective responses in V4 (Desimone & Schein, 1987; Ferrera et al., 1994; Gur & Snodderly, 2007; Roe et al., 2012) as well as evidence for dynamic or plastic effects in which motion responses emerge in V4 neurons after motion adaptation (Tolias, Keliris, Smirnakis, & Logothetis, 2005) or after disruption by V1 lesions (Schmid et al., 2013). Our findings support the causal involvement of V4 in motion processing and favor a more distributed circuit indicative of functional overlap between regions, challenging the view that dorsal regions alone contribute to motion perception. Ventral visual cortex may be an active contributor to motion perception with independent motion processing occurring within the each of the two areas. Motion information, for instance, may need to be processed in different ways to serve different purposes. Dorsal regions may drive the processing of visual motion leading to action, whereas ventral regions may contribute to visual motion leading to perception (Goodale & Milner, 1992). Alternatively, ventral stream regions may simply be recipients of feed-forward and feedback inputs from motion-selective regions via parallel and/or serial connections with areas such as hMT+ (Maunsell & Van Essen, 1983a; Ungerleider & Desimone, 1986).

A degree of flexibility and plasticity is already known to exist between visual cortical areas, supporting a more fluid breakdown of function between cortical sites. For example, prior training on motion tasks has been shown, in both human and nonhuman primates, to modify functional specialization within visual cortex by shifting the functional involvement between MT and V3A, depending on the training history and type of

stimulus, in an adaptive and flexible way (Chen, Cai, Zhou, Thompson, & Fang, 2016; Liu & Pack, 2017). Our results suggest that motion perception may be a distributed process not limited to dorsal regions and instead reflects the action and interaction of multiple neuronal systems within extrastriate cortex.

The role of hV4 in contrast perception and orientation discrimination

Compared to the body of work exploring the effects of rTMS on motion perception, the effect of rTMS on static, form-based tasks has been explored very little. Silson et al. (2013) demonstrate a double dissociation between VF maps LO1 and LO2 for the processing of orientation and shape, respectively, whereby rTMS to LO1 disrupts orientation (but not shape) discrimination and rTMS to LO2 disrupts shape (but not orientation) discrimination, suggesting that rTMS can selectively impact performance on nonmotion tasks. Here, by showing differential changes in performance on contrast increments and decrements, we have demonstrated a significant loss in perceived contrast following stimulation of hV4 and hMT+ for stimuli presented in the contralateral VF with the larger effect found for stimulation of hV4. Although rTMS and different forms of electrical transcranial brain stimulation (DCS and tRANS) have been shown to impact contrast sensitivity in clinical populations (B. Thompson, Mansouri, Koski, & Hess, 2008; Spiegel, Byblow, Hess, & Thompson, 2013) and enhance perceptual training in clinical populations on contrast-based tasks (Camilleri, Pavan, Ghin, Battaglini, & Campana, 2014; Campana, Camilleri, Pavan, Veronese, & Lo Giudice, 2014), this is, to our knowledge, the first time that rTMS has been shown to affect contrast perception directly in normal participants. Our results show a deficit of contrast perception compared to the enhancement reported in the clinical studies cited above and are consistent with the primate literature, which has shown area V4 to play a principal role in contrast detection and discrimination (Schiller & Lee, 1991).

Contrary to the results of Silson et al. (2013) for area LO1, we find no effect of rTMS on the ability to perform the orientation-discrimination task for which we collected pilot data, suggesting that this task is not functionally mediated by hV4. The orientation discrimination of a multielement population with a high orientation variance was chosen to be similar to the multielement motion-discrimination task. However, tasks that involve contours, curves, or other shapes may prove more suitable for targeting hV4 function as they are better related to the properties of V4 neurons (Pasupathy & Connor, 1999).

The role of hMT+ in static contrast perception

Our results have shown an involvement of hMT+ in contrast perception, specific to the contralateral VF. Primate data also show a small deficit in contrast thresholds in contralateral but not ipsilateral VF when MT is lesioned (Newsome & Pare, 1988). The effects observed for stimulation of hMT+ may be mediated by direct impairment of functional contrast perception in hMT+ in line with a role of MT neurons in various aspects of static contrast perception (T. D. Albright, 1984). rTMS suggests that involvement of hMT+ in global spatial tasks for static stimuli is unlikely (Pavan et al., 2017). It is possible that the effect of rTMS on contrast perception is mediated by ventral regions via some form of cortical cross-connectivity in line with the observation that direct stimulation of hV4 produces the larger effect. Whether the effects are mediated by connectivity with hV4 or by a direct involvement of hMT+ in contrast discrimination, this result is counter to the idea that hMT+ has no role in the perception of static stimulus contrast.

Spatial selectivity of rTMS effects

To make definitive claims about the functional roles played by areas hMT+ and hV4 in the processing of motion and form, it is necessary to demonstrate that perceptual effects are specific to the task and the cortical region being stimulated. The absence of any effect on the orientation-discrimination task (Figure 6) or motion discrimination for ipsilateral V4 (Figure 3) suggests that there is selectivity for the types of tasks affected by rTMS in these areas. This is consistent with the results of McKeefry et al. (2008), who demonstrate that the same rTMS protocols affecting motion perception did not impair the processing of spatial frequency. These are useful controls in that they rule out the possibility that a loss of performance may be due to the nonspecific effects of magnetic stimulation, such as discomfort and/or twitching generated by stimulation of facial nerves. That discomfort is not a significant factor is further supported by the consistent lack of effect following stimulation of hV4 for stimuli presented in the ipsilateral VF.

We have considered whether perceptual effects attributed to indirect disruption of functional connectivity between hMT+ and hV4 might instead result from the passive spread of rTMS across the cortical surface. Although local spread of magnetic field is unavoidable across tissue adjacent to target sites, previous work has demonstrated that the differential effects of TMS are measurable in targets with centroids as close as 10 mm apart (Pitcher, Charles, Devlin, Walsh, & Duchaine, 2009; Silson et al., 2013; Strong et

Subject	hMT+			hV4			Distance (mm)
	x	*y*	*z*	*x*	*y*	*z*	
S1	−48	51	0	−26	72	−18	20.9
S2	−50	61	−24	−30	80	−38	25.8
S3	−43	73	−10	−22	81	−23	26.0
S4	45	74	5	29	85	−12	27.0
S5	−39	59	−27	−20	64	−34	30.9
S6	30	69	−25	50	61	−2	31.5
S7	48	57	−8	39	62	−33	35.3

Table 2. Coordinates for areas hMT+ and hV4 for each of the seven participants as well as distance between hMT+ and hV4 stimulation sites. *Note*: The *x*, *y*, and *z* coordinates indicate distance (mm, in native space) along the right-to-left (−*x* to *x*), anterior-to-posterior (−*y* to *y*), and inferior-to-superior (−*z* to *z*) axes relative the participant's anterior commissure.

al., 2017a). For all our subjects, the distance between hMT+ and hV4 was greater than 20 mm apart (see Table 2). Additional controls for the lateral spread of rTMS effects are often performed by moving the coil 1–2 cm from the primary site of stimulation. We found that stimulating a different site the same distance from hMT+ as hV4 but in a different direction induced no significant deficits in performance in our control experiment (Figure 7). In addition, we find that the impairment in performance with hV4 stimulation for the motion-based tasks shows no decrease with increased distance of this area from hMT+ across subjects (Figure 8A), further excluding the possibility that the common effects observed between areas are due to the local spread of rTMS. Finally, we find that, across all tasks, a positive correlation exists between the magnitude of effect sizes in hMT+ and those in hV4 (Figure 8B), further supporting the role of functional connectivity between hMT+ and hV4, whereby stimulation of one automatically affects the other, possibly mediated through connections between dorsal and ventral cortex. The ventral part of area V3 lies posteriorly adjacent to V4 at this eccentricity (Figure 1A), and hence, we cannot rule out an effect of passive spread of V4 stimulation into this area. V3 represents one stage lower (earlier) in a continuous transformation of visual processing along the ventral pathway and may potentially contribute to some of the effects we find, such as a loss of perceived contrast, motion slowing, and loss of coherence. Nevertheless, these would still reflect cross-functional effects between dorsal and ventral specializations.

Conclusions

This study demonstrates that measurable and task-specific deficits arise following rTMS to areas hMT+ and hV4. rTMS to areas hMT+ and hV4 impairs performance on direction discrimination and produces differential changes in the discrimination of speed increments and decrements that demonstrate a perceptual slowing of the stimuli. Stimulation of hMT+ leads to bilateral impairments (in both VFs), whereas rTMS to hV4 leads to impairments only in the contralateral VF, showing that area hMT+ has a bilateral VF representation for motion-based tasks. We also find that rTMS to both areas leads to a loss in perceived contrast for stimuli presented in the contralateral VF with the greatest effect for hV4 stimulation. Thus, there is strong evidence for functional crossover

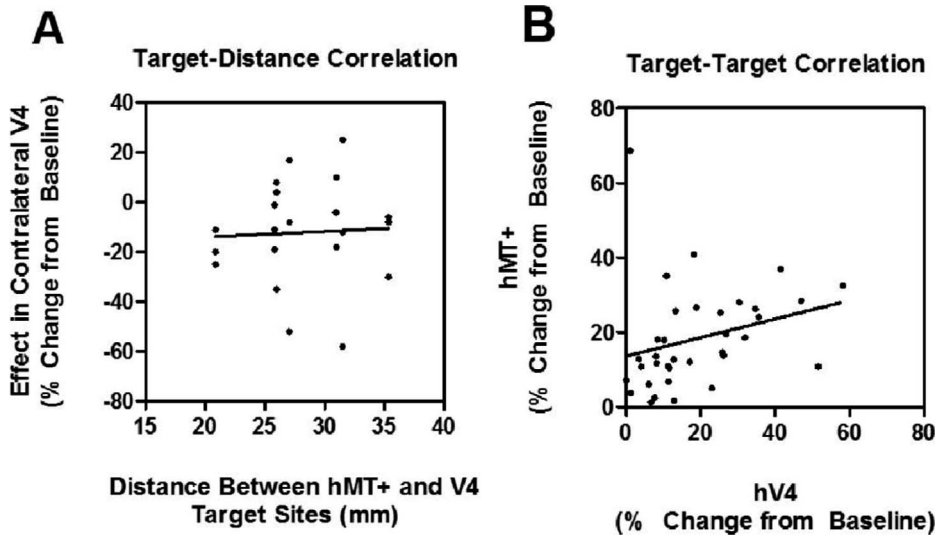

Figure 8. Task-averaged plots showing correlation between (A) effect size in area hV4 for stimuli presented in the contralateral VF (*y*-axis) versus distance between target sites (*x*-axis) and (B) effect size in area hMT+ (*y*-axis) versus area hV4 (*x*-axis). Data points throughout represent performance measured as percentage change from baseline for each of the individual subjects.

with hV4 involved in motion tasks and hMT+ in static contrast perception only in the contralateral VF, supporting a convergence of function between dorsal and ventral cortical regions.

Keywords: human vision, motion perception, contrast perception, form perception, repetitive transcranial magnetic stimulation (rTMS), hV4, hMT+

Acknowledgments

We thank Dr. Robert Hess for helpful discussion and Dr. Alexandre Renaud for his assistance with TMS experiments. We also thank our subjects for their participation in this study and Irem Nur Onay for her contributions to the early stages of this work. Supported by the Natural Sciences and Engineering Research Council (grant RGPIN 183625-05) and the Canadian Institutes of Health Research (grant MOP-10891) to KTM.

Commercial relationships: none.
Corresponding author: Kathy T. Mullen.
Email: kathy.mullen@mcgill.ca.
Address: McGill Vision Research, Department of Ophthalmology, McGill University, Montreal, Quebec, Canada.

References

Ajina, S., Pestilli, F., Rokem, A., Kennard, C., & Bridge H. (2015). Human blindsight is mediated by an intact geniculo-extrastriate pathway. *Elife 4*: e08935.

Albright, T., & Desimone, R. (1987). Local precision of visuotopic organization in the middle temporal area (MT) of the macaque. *Experimental Brain Research*, *65*(3), 582–592.

Albright, T. D. (1984). Direction and orientation selectivity of neurons in visual area MT of the macaque. *Journal of Neurophysiology*, *52*(6), 1106–1130.

Amano, K., Wandell, B. A., & Dumoulin, S. O. (2009). Visual field maps, population receptive field sizes, and visual field coverage in the human MT+ complex. *Journal of Neurophysiology*, *102*(5), 2704–2718.

An, X., Gong, H., Qian, L., Wang, X., Pan, Y., Zhang, X., ... Wang, W. (2012). Distinct functional organizations for processing different motion signals in V1, V2, and V4 of macaque. *Journal of Neuroscience*, *32*(39), 13363–13379.

Benjamini, Y., & Hochberg, Y. (1995). Controlling the false discovery rate: A practical and powerful approach to multiple testing. *Journal of the Royal Statistical Society. Series B (Methodological)*, *57*(1), 289–300.

Born, R. T., & Bradley, D. C. (2005). Structure and function of visual area MT. *Annual Review of Neuroscience*, *28*, 157–189.

Brainard, D. H. (1997). The psychophysics toolbox. *Spatial Vision*, *10*, 433–436.

Camilleri, R., Pavan, A., Ghin, F., Battaglini, L., & Campana, G. (2014). Improvement of uncorrected visual acuity and contrast sensitivity with perceptual learning and transcranial random noise stimulation in individuals with mild myopia. *Frontiers in Psychology*, *5*: 1234.

Campana, G., Camilleri, R., Pavan, A., Veronese, A., & Lo Giudice, G. (2014). Improving visual functions in adult amblyopia with combined perceptual training and transcranial random noise stimulation (tRNS): A pilot study. *Frontiers in Psychology*, *5*: 1402.

Chen, N., Cai, P., Zhou, T., Thompson, B., & Fang, F. (2016). Perceptual learning modifies the functional specializations of visual cortical areas. *Proceedings of the National Academy of Sciences, USA*, *113*(20), 5724–5729.

Cohen, J. (1988). *Statistical Power Analysis for the Behavioral Sciences*. Hillsdale, NJ: Lawrence Erlbaum.

Cowey, A., Campana, G., Walsh, V., & Vaina, L. M. (2006). The role of human extra-striate visual areas V5/MT and V2/V3 in the perception of the direction of global motion: A transcranial magnetic stimulation study. *Experimental Brain Research*, *171*(4), 558–562.

Cox, R. W. (1996). AFNI: Software for analysis and visualization of functional magnetic resonance neuroimages. *Computers and Biomedical Research*, *29*(3), 162–173.

Dale, A. M., Fischl, B., & Sereno, M. I. (1999). Cortical surface-based analysis. I. Segmentation and surface reconstruction. *Neuroimage*, *9*(2), 179–194.

Desimone, R., & Schein, S. J. (1987). Visual properties of neurons in area V4 of the macaque: Sensitivity to stimulus form. *Journal of Neurophysiology*, *57*(3), 835–868.

Dukelow, S. P., DeSouza, J. F., Culham, J. C., van den Berg, A. V., Menon, R. S., & Vilis, T. (2001). Distinguishing subregions of the human MT+

complex using visual fields and pursuit eye movements. *Journal of Neurophysiology*, *86*(4), 1991–2000.

Engel, S. A., Rumelhart, D. E., Wandell, B. A., Lee, A. T., Glover, G. H., Chichilnisky, E. J., & Shadlen, M. N. (1994, June 16). fMRI of human visual cortex. *Nature*, *369*(6481), 525.

Ferrera, V. P., Nealey, T. A., & Maunsell, J. (1994). Responses in macaque visual area V4 following inactivation of the parvocellular and magnocellular LGN pathways. *Journal of Neuroscience*, *14*(4), 2080–2088.

Fischl, B., Sereno, M. I., & Dale, A. M. (1999). Cortical surface-based analysis. II: Inflation, flattening, and a surface-based coordinate system. *Neuroimage*, *9*(2), 195–207.

Gallant, J. L., Braun, J., & Van Essen, D. C. (1993, January 1). Selectivity for polar, hyperbolic, and Cartesian gratings in macaque visual cortex. *Science*, *259*(5091), 100–103.

Gilaie-Dotan, S., Saygin, A. P., Lorenzi, L. J., Egan, R., Rees, G., & Behrmann, M. (2013). The role of human ventral visual cortex in motion perception. *Brain*, *136*(Pt. 9), 2784–2798.

Goodale, M. A., & Milner, A. D. (1992). Separate visual pathways for perception and action. *Trends in Neurosciences*, *15*(1), 20–25.

Gur, M., & Snodderly, D. M. (2007). Direction selectivity in V1 of alert monkeys: Evidence for parallel pathways for motion processing. *The Journal Physiology*, *585*(Pt. 2), 383–400.

Hayward, J., Truong, G., Partanen, M., & Giaschi, D. (2011). Effects of speed, age, and amblyopia on the perception of motion-defined form. *Vision Research*, *51*(20), 2216–2223.

Huk, A. C., Dougherty, R. F., & Heeger, D. J. (2002). Retinotopy and functional subdivision of human areas MT and MST. *Journal of Neuroscience*, *22*(16), 7195–7205.

Kaderali, S., Kim, Y. J., Reynaud, A., & Mullen, K. T. (2015). The role of human brain area hMT+ in the perception of global motion investigated with repetitive transcranial magnetic stimulation (rTMS). *Brain Stimulation*, *8*(2), 200–207.

Khawaja, F. A., Liu, L. D., & Pack, C. C. (2013). Responses of MST neurons to plaid stimuli. *Journal of Neurophysiology*, *110*(1), 63–74.

Komatsu, H., & Wurtz, R. H. (1988). Relation of cortical areas MT and MST to pursuit eye movements. I. Localization and visual properties of neurons. *Journal of Neurophysiology*, *60*(2), 580–603.

Larsson, J., & Heeger, D. J. (2006). Two retinotopic visual areas in human lateral occipital cortex. *Journal of Neuroscience*, *26*(51), 13128–13142.

Leh, S. E., Ptito, A., Schönwiesner, M., Chakravarty, M. M., & Mullen, K. T. (2010). Blindsight mediated by an S-cone-independent collicular pathway: An fMRI study in hemispherectomized subjects. *Journal of Cognitive Neuroscience*, *22*(4), 670–682.

Li, P., Zhu, S., Chen, M., Han, C., Xu, H., Hu, J., ... Lu, H. D. (2013). A motion direction preference map in monkey V4. *Neuron*, *78*(2), 376–388.

Liu, L. D., & Pack, C. C. (2017). The contribution of area MT to visual motion perception depends on training. *Neuron*, *95*(2), 436–446. e433.

Lu, H. D., Chen, G., Tanigawa, H., & Roe, A. W. (2010). A motion direction map in macaque V2. *Neuron*, *68*(5), 1002–1013.

Mansouri, B., Hess, R. F., & Allen, H. A. (2007). Orientation variance discrimination in amblyopia. *Journal of the Optical Society of America A, Optics, Image Science, and Vision*, *24*(9), 2499–2504.

Maunsell, J., & Van Essen, D. C. (1983a). The connections of the middle temporal visual area (MT) and their relationship to a cortical hierarchy in the macaque monkey. *Journal of Neuroscience*, *3*(12), 2563–2586.

Maunsell, J. H., & Van Essen, D. C. (1983b). Functional properties of neurons in middle temporal visual area of the macaque monkey. II. Binocular interactions and sensitivity to binocular disparity. *Journal of Neurophysiology*, *49*(5), 1148–1167.

McKeefry, D. J., Burton, M. P., & Morland, A. (2010). The contribution of human cortical area V3A to the perception of chromatic motion: A transcranial magnetic stimulation study. *European Journal of Neuroscience*, *31*(3), 575–584.

McKeefry, D. J., Burton, M. P., Vakrou, C., Barrett, B. T., & Morland, A. B. (2008). Induced deficits in speed perception by transcranial magnetic stimulation of human cortical areas V5/MT+ and V3A. *Journal of Neuroscience*, *28*(27), 6848–6857.

Michna, M. L., & Mullen, K. T. (2008). The contribution of color to global motion processing. *Journal of Vision*, *8*(5):10, 1–12, https://doi.org/10.1167/8.5.10. [PubMed] [Article]

Mullen, K. T., Dumoulin, S. O., McMahon, K. L., De Zubicaray, G. I., & Hess, R. F. (2007). Selectivity of human retinotopic visual cortex to S–cone–opponent, L/M–cone–opponent and achromatic stimulation. *European Journal of Neuroscience*, *25*(2), 491–502.

Mullen, K. T., Thompson, B., & Hess, R. F. (2010). Responses of the human visual cortex and LGN to achromatic and chromatic temporal modulations: An fMRI study. *Journal of Vision*, *10*(13):13, 1–19, https://doi.org/10.1167/10.13.13. [PubMed] [Article]

Mullen, K. T., Yoshizawa, T., & Baker, C. L., Jr. (2003). Luminance mechanisms mediate the motion of red–green isoluminant gratings: The role of temporal chromatic aberration. *Vision Research*, *43*(11), 1237–1249.

Newsome, W. T. (1997). Deciding about motion: Linking perception to action. *Journal of Comparative Physiology A*, *181*(1), 5–12.

Newsome, W. T., & Pare, E. B. (1988). A selective impairment of motion perception following lesions of the middle temporal visual area (MT). *Journal of Neuroscience*, *8*(6), 2201–2211.

O'Craven, K. M., Rosen, B. R., Kwong, K. K., Treisman, A., & Savoy, R. L. (1997). Voluntary attention modulates fMRI activity in human MT-MST. *Neuron*, *18*(4), 591–598.

Pasupathy, A., & Connor, C. E. (1999). Responses to contour features in macaque area V4. *Journal of Neurophysiology*, *82*(5), 2490–2502.

Pavan, A., Ghin, F., Donato, R., Campana, G., & Mather, G. (2017). The neural basis of form and form-motion integration from static and dynamic translational Glass patterns: A rTMS investigation. *Neuroimage*, *157*, 555–560.

Pelli, D. G. (1997). The VideoToolbox software for visual psychophysics: Transforming numbers into movies. *Spatial Vision*, *10*(4), 437–442.

Pitcher, D., Charles, L., Devlin, J. T., Walsh, V., & Duchaine, B. (2009). Triple dissociation of faces, bodies, and objects in extrastriate cortex. *Current Biology*, *19*(4), 319–324.

Roe, A. W., Chelazzi, L., Connor, C. E., Conway, B. R., Fujita, I., Gallant, J. L., … Vanduffel, W. (2012). Toward a unified theory of visual area V4. *Neuron*, *74*(1), 12–29.

Rust, N. C., Mante, V., Simoncelli, E. P., & Movshon, J. A. (2006). How MT cells analyze the motion of visual patterns. *Nature Neuroscience*, *9*(11), 1421–1431.

Saad, Z. S., Reynolds, R. C., Argall, B., Japee, S., & Cox, R. W. (2004). SUMA: An interface for surface-based intra-and inter-subject analysis with AFNI. In *Biomedical Imaging: Nano to Macro, 2004. IEEE International Symposium on, IEEE* (pp. 1510–1513). Washington, DC: IEEE.

Saad, Z. S., Ropella, K. M., Cox, R. W., & DeYoe, E. A. (2001). Analysis and use of FMRI response delays. *Human Brain Mapping*, *13*(2), 74–93.

Schiller, P. H., & Lee, K. (1991, March 8). The role of the primate extrastriate area V4 in vision. *Science*, *251*(4998), 1251–1253.

Schmid, M. C., Schmiedt, J. T., Peters, A. J., Saunders, R. C., Maier, A., & Leopold, D. A. (2013). Motion-sensitive responses in visual area V4 in the absence of primary visual cortex. *Journal of Neuroscience*, *33*(48), 18740–18745.

Sereno, M. I., Dale, A., Reppas, J., Kwong, K., Belliveau, J., Brady, T., … Tootell, R. (1995, May 12). Borders of multiple visual areas in humans revealed by functional magnetic resonance imaging. *Science*, *268*(5212), 889–893.

Silson, E. H., McKeefry, D. J., Rodgers, J., Gouws, A. D., Hymers, M., & Morland, A. B. (2013). Specialized and independent processing of orientation and shape in visual field maps LO1 and LO2. *Nature Neuroscience*, *16*(3), 267–269.

Spiegel, D. P., Byblow, W. D., Hess, R. F., & Thompson, B. (2013). Anodal transcranial direct current stimulation transiently improves contrast sensitivity and normalizes visual cortex activation in individuals with amblyopia. *Neurorehabilitation and Neural Repair*, *27*(8), 760–769.

Stevens, L. K., McGraw, P. V., Ledgeway, T., & Schluppeck, D. (2009). Temporal characteristics of global motion processing revealed by transcranial magnetic stimulation. *The European Journal of Neuroscience*, *30*(12), 2415–2426.

Strong, S. L., Silson, E. H., Gouws, A. D., Morland, A. B., & McKeefry, D. J. (2017a). A direct demonstration of functional differences between subdivisions of human V5/MT. *Cerebral Cortex*, *27*(1), 1–10.

Strong, S. L., Silson, E., Gouws, A., Morland, A., & McKeefry, D. (2017b). Ipsilateral sensitivity to visual motion is restricted to V5/MT+ in the right cerebral hemisphere. *Journal of Vision*, *17*(10):607, https://doi.org/10.1167/17.10.607. [Article]

Thakral, P. P., & Slotnick, S. D. (2011). Disruption of MT impairs motion processing. *Neuroscience Letters*, *490*(3), 226–230.

Thompson, B., Mansouri, B., Koski, L., & Hess, R. F. (2008). Brain plasticity in the adult: Modulation of function in amblyopia with rTMS. *Current Biology*, *18*(14), 1067–1071.

Thompson, P., Brooks, K., & Hammett, S. T. (2006). Speed can go up as well as down at low contrast: Implications for models of motion perception. *Vision Research*, *46*(6–7), 782–786.

Tolias, A. S., Keliris, G. A., Smirnakis, S. M., & Logothetis, N. K. (2005). Neurons in macaque area V4 acquire directional tuning after adaptation to motion stimuli. *Nature Neuroscience*, *8*(5), 591–593.

Tolias, A. S., Sultan, F., Augath, M., Oeltermann, A., Tehovnik, E. J., Schiller, P. H., & Logothetis, N. K. (2005). Mapping cortical activity elicited with electrical microstimulation using FMRI in the macaque. *Neuron*, *48*(6), 901–911.

Ungerleider, L. G., & Desimone, R. (1986). Cortical connections of visual area MT in the macaque. *Journal of Comparative Neurology*, *248*(2), 190–222.

Walsh, V., Ellison, A., Battelli, L., & Cowey, A. (1998). Task-specific impairments and enhancements induced by magnetic stimulation of human visual area V5. *Proceedings of the Royal Society of London B: Biological Sciences*, *265*(1395), 537–543.

Wassermann, E. M. (1998). Risk and safety of repetitive transcranial magnetic stimulation: Report and suggested guidelines from the International Workshop on the Safety of Repetitive Transcranial Magnetic Stimulation, June 5–7, 1996. *Electroencephalography and Clinical Neurophysiology/Evoked Potentials Section*, *108*(1), 1–16.

Waterston, M. L., & Pack, C. C. (2010). Improved discrimination of visual stimuli following repetitive transcranial magnetic stimulation. *PLoS One*, *5*(4), e10354.

Yue, X., Pourladian, I. S., Tootell, R. B., & Ungerleider, L. G. (2014). Curvature-processing network in macaque visual cortex. *Proceedings of the National Academy of Sciences, USA*, *111*(33), E3467–E3475.

Zeki, S. M. (1974). Functional organization of a visual area in the posterior bank of the superior temporal sulcus of the rhesus monkey. *The Journal of Physiology*, *236*(3), 549–573.